ISBN: 978-3-95450-230-1 ISSN: 2673-5350 doi:10.18429/JACoW-IBIC2021-TUPP19

PROPOSED RESEARCH WITH MICROBUNCHED BEAMS AT LEA*

A. H. Lumpkin†, Argonne Associate, Argonne National Laboratory, Lemont, IL 60439 USA
W. J. Berg, J. Dooling, Y. Sun, K.P. Wootton, Argonne National Laboratory, Lemont, IL 60439 USA
D. W. Rule, Silver Spring, MD, 20904 USA
A. Murokh, RadiaBeam Technologies LLC, Santa Monica, CA 90404 USA
P. Musumeci, UCLA, Los Angeles, CA 90095 USA

Abstract

Significant microbunching of an electron beam at 266 nm is projected with the co-propagation of electrons at 375 MeV and a UV laser pulse through a 3.2-cm period prebuncher undulator. Such microbunched beams will generate coherent optical transition radiation at a metal screen surface boundary or coherent optical diffraction radiation from a nearby metal surface (new model presented). With a 10% microbunching fraction, coherent enhancements of more than 7 million are modelled for a 300-pC charge. Diagnostic plans are described for beam size, divergence, electron microbunching fraction, spectrum, and bunch length on a single shot at the Argonne National Laboratory Linac Extension Area (LEA).

INTRODUCTION

One of the advantages of relativistic electron beams with microbunching at UV to visible wavelengths is the potential to generate coherent optical transition radiation (COTR) at a metal foil for diagnostics purposes. A significant microbunching fraction of at least 10% is expected for the case of a seed laser at 266 nm copropagating with a 375-MeV electron beam through a modulator undulator (3.2 cm period) at the Linac Extension Area (LEA) at Argonne National Laboratory [1,2]. Diagnostic plans have been made for the COTR-based characterization of the microbunched beam size (~100 microns), divergence (sub-mrad), microbunching fraction, spectrum, and bunch length (sub-ps), as well as coalignment of the laser pulse and electron beam as previously described [3]. For that case, COTR enhancements over OTR of more than seven million were calculated, and we expect a similar enhancement of coherent optical diffraction radiation (CODR). Thus, we propose the modification of the microbunching diagnostics station to support initial CODR experiments with beam transit through an aperture in a metal screen or near a metal edge at the second screen position of the interferometer. We would explore whether the coherence function for CODR provides a complementary beam size monitor.

EXPERIMENTAL ASPECTS

The Advanced Photon Source (APS) linac includes options for injection of beam from either a thermionic cathode (TC) rf gun or a photocathode (PC) rf gun into an S-band linac with final beam energies of up to 500 MeV. The schematic of the facility is given in Fig. 1. For operations providing beam to the APS storage ring, beam from one of the two thermionic guns is used. For these proposed experiments, single micropulses from the PC rf gun with Cu cathode irradiated by a quadrupled Nd glass laser at 2 or 6 Hz would be used with electron beam parameters given in Table 1. The chicane is used for bunch compression from 2 ps down to σ_t ~0.5 ps.

At the end of the linac there is an option to transport beam with a bypass of the Particle Accumulator Ring (PAR) to the LEA building where the experiments can be performed. A schematic of the experimental geometry is shown in Fig. 2. After the modulator and dispersive section, there would be the diagnostics chamber which is repurposed from a previous FEL experiment [4]. This chamber has stepper actuators at two locations in z separated by 6.3 cm. The first is a normal imaging station with positions for a YAG:Ce screen plus 45-degree mirror or a metal foil at 45 degrees. When this latter 10-μm thick Al foil is selected, it blocks the seed laser, and it also generates forward COTR as the beam exits from the back surface in the direction of the second mirror at 45 degrees which is 6.3 cm downstream. COTR is also generated at the front surface of this metal mirror. The combination of sources provides the COTR interferometry. By using near field (NF) focusing the microbunched beam size at the first screen can be measured, and by using far-field (FF) focusing the angular distribution pattern of the COTR interferences can be seen and divergences assessed. The expected COTRI patterns have been previously reported [3,5], and an example is provided in the next section.

The YAG:Ce emissions are near 550 nm so a standard digital CMOS camera would be used for initial beam size imaging. The COTR and CODR would be narrowband at the wavelength of the UV seed laser so a UV sensitive imager is needed with a digital capability preferred. Multiple cameras would be used with beam splitters to provide NF, FF, polarized imaging, and spectra on a single shot for

Table 1: Linac Parameters for PC Gun Beam Used in the Proposed Tests

Parameter	Units	Value
Energy	MeV	375
Charge	pC	100-300
Emittance	mm mrad	2-4
Bunch length	ps	0.5-2.0

* Work supported in part by UChicago Argonne, LLC under Contract No. DE-AC02-07CH11357 with the U.S. Department of Energy, Office of Science, Office of Basic Energy Sciences.
† lumpkin@anl.gov

ISBN: 978-3-95450-230-1 ISSN: 2673-5350 doi:10.18429/JACoW-IBIC2021-TUPP19

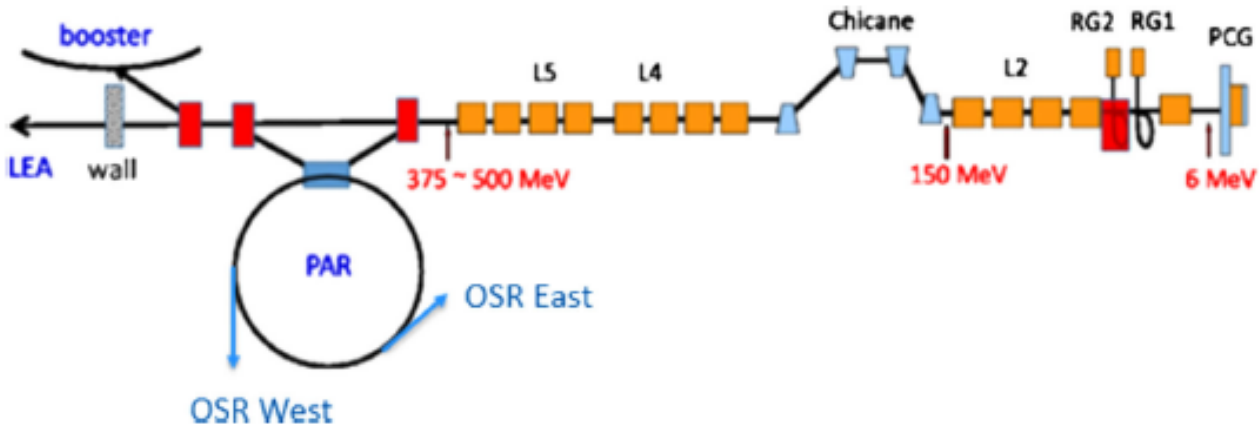

Figure 1: Schematic of the APS linac showing the PC rf gun (PCG), two thermionic cathode rf guns (RG1 and RG2), the accelerating structures (L2, L4, L5), the chicane, PAR, and transport to the LEA. A beam interleaving scheme allows the use of PC gun beam for LEA when the RG2 beam is not needed for the PAR, booster, and storage ring.

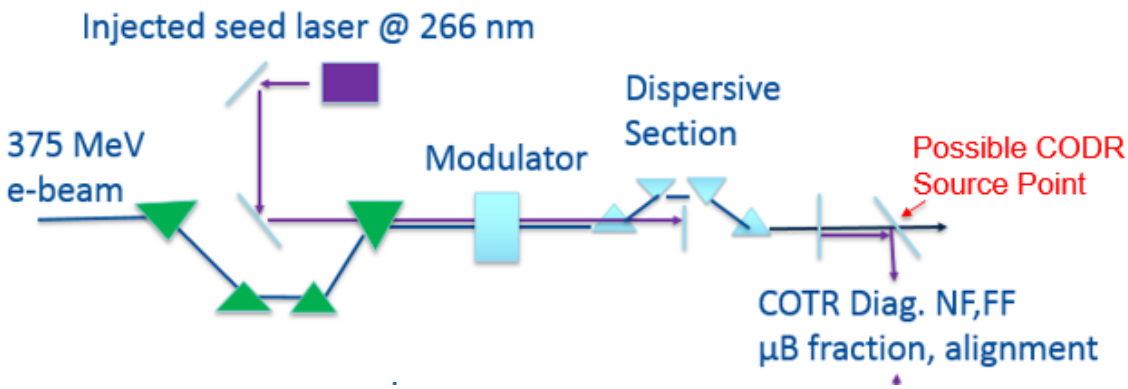

Figure 2: Schematic of the proposed experiment in the LEA showing the seed laser injection point, modulator, dispersive section, and the microbunching diagnostics station for COTR and CODR measurements.

COTR. The spectrometer readout would be done with another UV camera. The microbunching fraction would be assessed by determining the ratio of observed COTR intensity with the seed laser in the modulator to OTR data obtained with the seed laser off as emitted from the back of the first screen. The use of a 450-nm long-pass filter would select the much weaker incoherent OTR for the total beam spot imaging. A UV-sensitive streak camera phase locked to 119 MHz could be used for the bunch length assessment at the sub-ps level. Alignment of the seed laser and electron beam can also be enabled by using the COTR-based transverse, angular, and longitudinal distributions.

The seed laser could be a commercially available Ti:Sapphire oscillator plus amplifier with frequency tripling to ~266 nm and with a nominal 300-fs bunch length after compression. This would be injected onto the beamline axis by mirrors for co-propagation with the electron beam through the modulator as indicated in Fig. 2.

MODELING ASPECTS

The two basic models for COTR and CODR are considered. They are extensions of the FF incoherent OTR Model and the NF ODR model reported previously [6, 7].

COTR Model

The COTR model was described in detail recently [6]. The screen positions act as a two-foil Wartski OTR interferometer [8] having foils at 45° to the beam axis and with spacing L=*63 mm*. The forward directed OTR from the first foil is reflected off the back of the second foil and interferes in the far field. We define the parallel and perpendicular polarizations for a scan along the θ_x axis.

To proceed we start with W_1, the number of OTR photons that a single electron generates per unit frequency ω per unit solid angle Ω from a single foil which is

$$\frac{d^2W_1}{d\omega d\Omega} = \frac{e^2}{\hbar c}\frac{1}{\pi^2\omega}\frac{(\theta_x^2+\theta_y^2)}{(\gamma^{-2}+\theta_x^2+\theta_y^2)^2}\,. \quad (1)$$

The COTRI model for the two-foil interferometer with the incoherent part $\propto N$ and the coherent part $\propto N_B^2$,

$$\frac{d^2W}{d\omega d\Omega} = \left|r_{\parallel,\perp}\right|^2 \frac{d^2W_1}{d\omega d\Omega}\,[N\boldsymbol{I}(\boldsymbol{k}) + N_B(N_B-1)\boldsymbol{J}(\boldsymbol{k})], \quad (2)$$

where N_B of the total number N are microbunched, i.e., the bunching fraction, bf= N_B /N. Here $\left|r_{\parallel,\perp}\right|^2$is the reflection coefficient for parallel or perpendicularly polarized OTR

ISBN: 978-3-95450-230-1 ISSN: 2673-5350 doi:10.18429/JACoW-IBIC2021-TUPP19

reflected from the *second* foil. ***I(k)*** is the expression for the interference of the OTR from the first and second foils of the interferometer, given by

$$\boldsymbol{I(k)} = 4\sin^2\left[\frac{kL}{4}\left(\gamma^{-2} + \theta_x^2 + \theta_y^2\right)\right], \qquad (3)$$

where $k = |\boldsymbol{k}| = 2\pi/\lambda$. Peaks of ***I(k)*** occur at angles ${\theta_x}^2 + {\theta_x}^2 = \frac{2\lambda}{L}(p - p_0)$, where $p = 1/2,\ 3/2\ \ldots$ and $p_0 = L/(2\lambda\gamma^2)$. For good sensitivity to divergence p_0 should be of order unity. The coherence function ***J(k)*** can be defined as

$$\boldsymbol{J(k)} = \left(H_1(\boldsymbol{k}) - H_2(\boldsymbol{k})\right)^2 + H_1(\boldsymbol{k})H_2(\boldsymbol{k})\boldsymbol{I(k)}, \quad (4)$$

where $H_j(\boldsymbol{k}) = \rho_j(\boldsymbol{k})/Q = g_j(k_x)\, g_j(k_y)\, F_z(k_z)$, for a microbunch of charge distribution $\rho_j(\boldsymbol{x})$ and total charge Q, with j = 1, 2. Here we have introduced two μ-bunch form factors, H_1 and H_2, to account for the increase in bunch radius from the first to the second interferometer foil due to beam divergence. This is important for micron sized beams, but it is a negligible effect for an initial 100-μm beam size with sub-mrad divergence considered here.

One prediction is that the coherence functions for 10 and 100 μm are quite different. As seen in Fig. 3a, only the inner lobes are enhanced for the 100-μm case so the cone angle is about ±1 mrad. The forward COTR will hit the intercepting mirror 63 mm away for COTRI, but it would miss the screen edge when located >200 μm away from the beam trajectory. This potentially allows one to image the CODR from the second screen in the near field. In Fig. 3b we show effects of divergence on COTRI fringe visibility for values of 0.1, 0.3, 0.5, and 0.7 mrad. The larger divergences reduce the modulation. The coherence function provides a 7-million intensity enhancement factor at the smaller angles.

CODR Model

Previously we employed incoherent ODR imaging as a non-intercepting diagnostic. Our initial NF ODR experiments were at 7 GeV on an extraction line from the Booster synchrotron at APS [7]. The high gamma allowed us to have an impact parameter of 4 σ_y above the beam for the horizontal lower edge of a Cu mirror surface. We were able to image the 1300-μm horizontal beam size with a 3 nC bunch charge. In the present case at gamma of ~734 and a beam size of 100 μm, we anticipate the incoherent ODR will be dramatically reduced by 2.6 x 10^{-6} at an impact parameter of 400 μm with λ= 266 nm. However, we estimate an enhancement of CODR to be about 7 x 10^6 for a 10% bunching fraction and micropulse charge of 300 pC as in COTR. We project the NF CODR would be detectable with a low-noise, 12-bit digital UV camera.

The necessity of relying on coherent ODR led us to develop a model for CODR which can be used to predict the enhancement and the effect of the μ-bunch's transverse and longitudinal structure. Our approach is based on the Weizächer-Williams's method of virtual quanta [9] which takes advantage of the similarity of a relativistic particle's

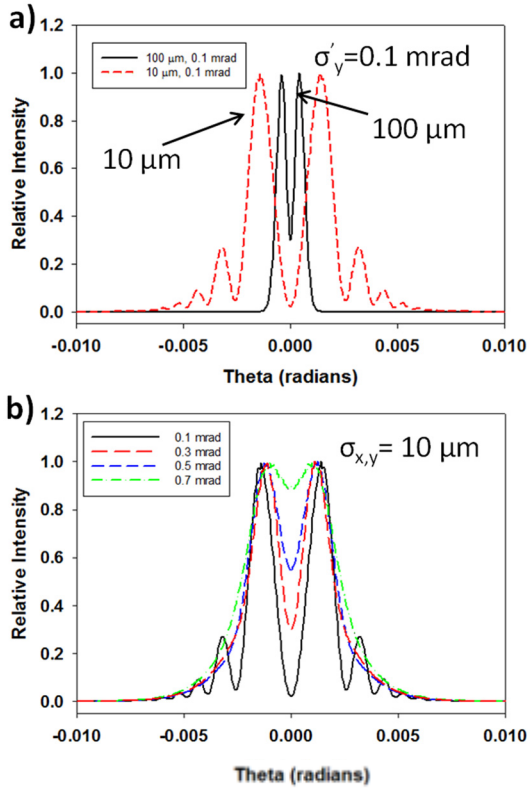

Figure 3: Plots of $I_{total} = I_{\parallel} + I_{\perp}$ for a) two beams with sizes $\sigma_{x,,y}$ =10 μm and 100 μm, both with divergence $\sigma'_{x,y}$=0.1 mrad, and b) beams all with size $\sigma_{x,y}$=10 μm and divergences $\sigma'_{x,y}$= 0,1, 0,3, 0,5 and 0.7 mrad. The common parameters used in a) and b) are E=375 MeV, 1/γ=1.36 mrad, L=63 mm, λ=266 nm, total charge=300 pC, and bunching fraction=10%.

field to a photon. The Fourier transform in time, t taken at an impact parameter b with respect to the particle's trajectory yields the frequency spectrum. Consider Fig. 4, a schematic of a metal screen with its edge at distance of e.g. ~ 4 σ_y, where the beam's vertical size is

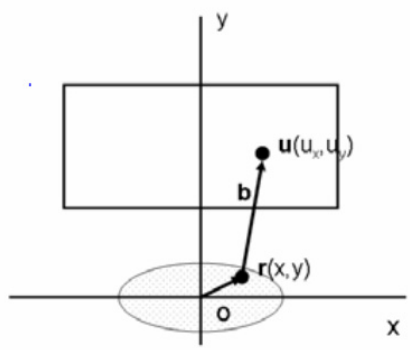

Figure 4: Schematic showing the transverse beam profile, ODR screen and vectors locating a beam particle and point P on the screen relative to the beam centroid [10].

~2 σ_y. An electron at $\boldsymbol{r_i}$ with respect to the beam centroid has an impact parameter $\boldsymbol{b_i}$ at point P in the screen, located by $\boldsymbol{u_i} = \boldsymbol{b_i} + \boldsymbol{r_i}$, as measured from the beam centroid. The backward ODR is proportional to the field strength squared

ISBN: 978-3-95450-230-1 ISSN: 2673-5350 doi:10.18429/JACoW-IBIC2021-TUPP19

and to the reflectance $|r_{\parallel,\perp}(\psi)|^2$ for parallel and perpendicular polarizations with the screen at angle ψ relative to the beam axis.

The frequency spectrum is given by [9]

$$\frac{dI(b_i,\omega)}{d\omega}(b_i,\omega) = \frac{c}{2\pi}|E_x(b_i,\omega)|^2 + \frac{c}{2\pi}|E_y(b_i,\omega)|^2, \quad (5)$$

where the electric field components polarized along the X- and Y-directions are [11]

$$E_{x,y}(b_i,\omega) = \frac{e\alpha}{\pi v}\, e^{-i\frac{\omega z}{v}} \frac{b_{ix,y}}{b_i} K_1(\alpha b_i)\,, \text{and } \omega = \boldsymbol{k}\cdot\boldsymbol{v}\,. \quad (6)$$

Here $\boldsymbol{b_i} = b_{ix}\hat{\boldsymbol{x}} + b_{iy}\hat{\boldsymbol{y}} = (u_x - x_i)\hat{\boldsymbol{x}} + (u_y - y_i)\hat{\boldsymbol{y}}$, and $\omega z/v = k_z z_i$, with z_i being parallel to $\boldsymbol{v}$. Also $K_1(\alpha b_i)$ is a modified Bessel function and $\alpha = \omega/v\gamma \approx 2\pi/\gamma\lambda$ for $v\sim c$.

If we have a beam which is partially μ-bunched with bunching fraction bf = N_B/N and charge $Q_B = N_B e$, we expect coherent ODR if the transverse beam sizes $\sigma_{x,y} \lesssim 2\pi/\gamma\lambda$ and the longitudinal size σ_z is such that $k_z\sigma_z\sim 1$.

The total frequency spectrum at point *P,* summing over all the electrons in a single μ-bunch is

$$\frac{dI^T(b_i,\omega)}{d\omega}(b_i,\omega) = \frac{c}{2\pi}|E_x^T(u,\omega)|^2 + \frac{c}{2\pi}|E_y^T(u,\omega)|^2, \quad (7)$$

where $E_{x,y}^T(u,\omega) = \sum_{i=1}^{N_B} E_{x,y}^i(b_i, z_i, \omega)$ and specializing to the y-polarization for simplicity, putting the explicit sums over particles in Eq. (7) above we have

$$\begin{aligned}|E_y^T(u,\omega)|^2 &= \sum_{i=1}^{N_B}\sum_{j=1}^{N_B} E_y^i E_y^{j^*} \\ &= \sum_{i=1}^{N_B}|E_y^i|^2 + \sum_{j\neq i}\sum_{i=1}^{N_B} E_y^i E_y^{j^*}\,. \end{aligned} \quad (8)$$

The first sum over *i*=*j* gives the incoherent ODR, while the sums over *i*=1-N_B and $i \neq j$ gives the coherent contribution.

This approach was also used for the COTR model, where we treated the μ-bunch as a product of normalized Gaussian forms, assuming that the x-, y-, and z-distributions are separable. The charge density is $\rho(x,y,z) = N_B e F_\parallel(z) F_\perp(x,y)$, with

$$\begin{aligned} F_\parallel(z) &= \frac{1}{\sqrt{2\pi\sigma_z^2}} e^{-z^2/2\sigma_z^2}\,, \\ F_\perp(x,y) &= \frac{1}{\sqrt{2\pi\sigma_x^2}}\frac{1}{\sqrt{2\pi\sigma_y^2}} e^{-x^2/2\sigma_x^2} e^{-y^2/2\sigma_y^2}. \end{aligned} \quad (9)$$

We now replace the incoherent sum over all *N* electrons by the following average of the intensity over the beam profile using Eq.(6):

$$\begin{aligned}\sum_{i=1}^{N_B}|E_y^i|^2 \rightarrow \langle|E_y(u,\omega)|^2\rangle = \\ N\frac{e^2\alpha^2}{\pi^2 v^2}\iint dxdy\frac{b_y^2}{b^2}K_1^2(\alpha b)F_\perp(x,y),\end{aligned} \quad (10)$$

where $b = \left[(u_x - x)^2 + (u_y - y)^2\right]^{1/2}$. Note that the *z*-dependent phase cancels for the sum over *i*=*j*. This incoherent model was used in Refs. [7, 10], with the integrals done numerically.

Next, we turn to the sums over *i*=1-N_B and $i \neq j$ for which there are $N_B(N_B-1)$ terms like $E_y^1(b_1,z_1,\omega)E_y^2(b_2,z_2,\omega)^*$. The impact parameters b_1 and b_2 for electrons 1 and 2 are independent variables and we further assume there is no correlation affecting the particles' separation $\boldsymbol{r}_1 - \boldsymbol{r}_2$. Again we proceed with the same Gaussian μ-bunch distribution, but now we average the field strength of each electron independently, rather than the intensity, as in the incoherent part above. We use the same form to do the averaging, given by

$$\begin{aligned}\langle E_y^i(u,\omega)\rangle = \\ \frac{e\alpha}{\pi v}\iiint dxdydze^{-ik_z z}F_\parallel(z)\frac{b_y}{b}K_1(\alpha b)F_\perp(x,y).\end{aligned} \quad (11)$$

Using the above averaging procedure we replace the sums over discrete electrons in the μ-bunch by

$$\begin{aligned}&N_B(N_B-1)\langle E_y^1(u,\omega)\rangle\langle E_y^2(u,\omega)\rangle^* = \\ &N_B(N_B-1)\frac{e^2\alpha^2}{\pi^2 v^2}e^{-(\sigma_z k_z)^2}\left|\iint dxdy\frac{b_y}{b}K_1(\alpha b)F_\perp(x,y)\right|^2.\end{aligned} \quad (12)$$

Here the integral of $e^{-ik_z z}F_\parallel(z)$ above in Eq. (11) gives the factor $e^{-(\sigma_z k_z)^2}$, the Fourier transform of the μ-bunch's longitudinal profile, indicating that the μ-bunch length should satisfy $k_z\sigma_z\sim 1$ for coherent ODR. The integral over the beam profile $F_\perp(x,y)$ will be done numerically, similarly to what was done in Refs. [7, 10]. The above Eq. (12) gives the coherent frequency spectrum when used in Eq. (7). The sum over a train of μ-bunches has been discussed in Ref. [4] and is omitted here because of space constraints.

The dependence on N_B^2 is the basis for the large enhancement of CODR expected in the present application, which will dominate the incoherent ODR for sufficiently large bunching fractions.

SUMMARY

In summary, we have described the potential for measuring a comprehensive set of microbunched electron beam properties on a single shot using COTR and potentially extending the basic techniques to CODR imaging. A new NF CODR model is described for the first time which will be used to guide future experiments.

ACKNOWLEDGEMENTS

The ANL-affiliated authors acknowledge the support of J. Byrd and M. Borland of the Accelerator Systems Division at ANL. The submitted manuscript has been created by UChicago Argonne, LLC, Operator of Argonne National Laboratory (Argonne). Argonne, a U.S. Department of Energy Office of Science Laboratory, is operated under Contract No. DE-AC02-06CH11357. The U.S. Government retains for itself, and others acting on its behalf, a paid-up nonexclusive, irrevocable worldwide license in said article to reproduce, prepare derivative works, distribute copies to the public, and perform publicly and display publicly, by or on behalf of the Government.

ISBN: 978-3-95450-230-1 ISSN: 2673-5350 doi:10.18429/JACoW-IBIC2021-TUPP19

REFERENCES

[1] W. Berg, J. C. Dooling, S. H. Lee, Y. Sun, and A. Zholents, "Development of the Linac Extension Area 450-MeV Electron Test Beam Line at the Advanced Photon Source", in *Proc. 8th Int. Beam Instrumentation Conf. (IBIC'19)*, Malmö, Sweden, Sep. 2019, pp. 219-221. doi:10.18429/JACoW-IBIC2019-MOPP048

[2] Y. Park *et al*., "Tapered helical undulator system for high efficiency energy extraction from a high brightness electron beam", submitted for publication.

[3] A. H. Lumpkin and D. W. Rule, "Feasibility of Single-Shot Microbunching Diagnostics for a Pre-Bunched Beam at 266 nm", in Proc. 39th Int. Free Electron Laser Conf. (FEL'19), Hamburg, Germany, Aug. 2019, pp. 408-411. doi:10.18429/JACoW-FEL2019-WEP041

[4] A. H. Lumpkin *et al.*, "Evidence for Microbunching "Sidebands" in a Saturated Free-Electron Laser Using Coherent Optical Transition Radiation," *Phys. Rev. Lett.*, vol. 88, no. 23, p. 234801, Jun. 2002. doi:10.1103/PhysRevLett.88.234801

[5] A. H. Lumpkin and D.W. Rule, "Single-shot Diagnostics of Microbunched Electrons in Laser-Driven Plasma Accelerators and Free-electron Lasers", in *Proc. 8th Int. Beam Instrumentation Conf. (IBIC'19)*, Malmö, Sweden, Sep. 2019, pp. 633-636. doi:10.18429/JACoW-IBIC2019-WEPP039

[6] A. H. Lumpkin *et al.*, "Coherent Optical Signatures of Electron Microbunching in Laser-Driven Plasma Accelerators," *Phys. Rev. Lett.*, vol. 125, no. 1, p. 014801, Jul. 2020. doi:10.1103/PhysRevLett.125.014801

[7] A. H. Lumpkin, W. J. Berg, N. S. Sereno, D. W. Rule, and C.-Y. Yao, "Near-field imaging of optical diffraction radiation generated by a 7-GeV electron beam," *Phys. Rev. ST Accel. Beams*, vol. 10, no. 2, p. 022802, Feb. 2007. doi:10.1103/PhysRevSTAB.10.022802

[8] L. Wartski *et al.*, "Interference phenomenon in optical transition radiation and its application to particle beam diagnostics and multiple-scattering measurements, *J. Appl. Phys. v*ol. 46, no. 8, p. 3644, Aug.1975. doi:10.1063/1.322092

[9] J. D. Jackson, "Bremsstrahlung, Method of Virtual Quanta, Radiative Beta Processes," in *Classical Electrodynamics*, 2nd ed., New York, NY, USA: Wiley, 1975.

[10] C.-Y. Yao, A. H. Lumpkin, and D. W. Rule, "Numerical Simulation of Optical Diffraction Radiation from a 7-GeV Beam", in *Proc. 22nd Particle Accelerator Conf. (PAC'07)*, Albuquerque, NM, USA, Jun. 2007, paper FRPMS001, pp. 3850-3852. doi:10.1109/PAC.2007.4440020

[11] M. L. Ter-Mikaelian, Electromagnetic Processes in Condensed Media, New York, NY, USA: Wiley-Interscience, 1972.